Loss of Macrophage Wnt Secretion Improves Remodeling and Function After Myocardial Infarction in Mice

Dahlia Palevski, MSc; La-Paz Levin-Kotler, MSc; David Kain, PhD; Nili Naftali-Shani, PhD; Natalie Landa, PhD; Tammy Ben-Mordechai, PhD; Tal Konfino, MSc; Radka Holbova, MSc; Natali Molotski, PhD; Rina Rosin-Arbesfeld, PhD; Richard A. Lang, PhD; Jonathan Leor, MD

Background—Macrophages and Wnt proteins (Wnts) are independently involved in cardiac development, response to cardiac injury, and repair. However, the role of macrophage-derived Wnts in the healing and repair of myocardial infarction (MI) is unknown. We sought to determine the role of macrophage Wnts in infarct repair.

Methods and Results—We show that the Wnt pathway is activated after MI in mice. Furthermore, we demonstrate that isolated infarct macrophages express distinct Wnt pathway components and are a source of noncanonical Wnts after MI. To determine the effect of macrophage Wnts on cardiac repair, we evaluated mice lacking the essential Wnt transporter *Wntless* (*Wls*) in myeloid cells. Significantly, *Wntless*-deficient macrophages presented a unique subset of M2-like macrophages with anti-inflammatory, reparative, and angiogenic properties. Serial echocardiography studies revealed that mice lacking macrophage Wnt secretion showed improved function and less remodeling 30 days after MI. Finally, mice lacking macrophage-*Wntless* had increased vascularization near the infarct site compared with controls.

Conclusions—Macrophage-derived Wnts are implicated in adverse cardiac remodeling and dysfunction after MI. Together, macrophage Wnts could be a new therapeutic target to improve infarct healing and repair. (*J Am Heart Assoc*. 2017;6:e004387. DOI: 10.1161/JAHA.116.004387.)

Key Words: macrophage • myocardial infarction • remodeling • Wnt signaling

D espite significant advances in cardiovascular medicine, optimization of myocardial repair and regeneration remains a major therapeutic challenge.[1] The immune system in general, and macrophages in particular, control the healing response after myocardial infarction (MI).[2-5] Macrophages are essential for the removal of necrotic tissue, resolution of inflammation, angiogenesis, scar formation, and regeneration.[2-7] Macrophages control these processes by

From the Neufeld Cardiac Research Institute, Sackler Faculty of Medicine (D.P., L.-P.L.-K., D.K., N.N.-S., N.L., T.B.-M., T.K., R.H., N.M., J.L.) and Department of Clinical Microbiology and Immunology, Sackler School of Medicine (R.R.-A.), Tel-Aviv University, Tel-Aviv, Israel; Tamman Cardiovascular Research Institute, Leviev Heart Center, Sheba Medical Center, Tel-Hashomer, Israel (D.P., L.-P.L.-K., D.K., N.N.-S., N.L., T.B.-M., T.K., R.H., N.M., J.L.); Sheba Center for Regenerative Medicine, Stem Cells and Tissue Engineering, Tel-Hashomer, Israel (D.P., L.-P.L.-K., D.K., N.N.-S., N.L., T.B.-M., T.K., R.H., N.M., J.L.); The Visual Systems Group Divisions of Pediatric Ophthalmology and Developmental Biology, Cincinnati Children's Hospital Medical Center Research Foundation, Cincinnati, OH (R.A.L.).

Correspondence to: Jonathan Leor, MD, Neufeld Cardiac Research Institute, Sheba Medical Center, Tel-Hashomer 52621, Israel. E-mail: leorj@post.tau.ac.il

the secretion of pro- and anti-inflammatory factors, angiogenic cytokines, and matrix metalloproteinases.[8-10] Furthermore, macrophages secrete Wnt ligands that can control tissue repair and regeneration.[11,12] Wnts are a family of 19 secreted glycoproteins that are essential for embryonic myocardial development and stem cell biology.[13] Wnts have also been implicated in response to cardiac stress and injury.[14-16] In general, the Wnt signaling pathway is divided into canonical (β-catenin dependent) and noncanonical (β-catenin independent) pathways. Several studies have shown that activation of the canonical Wnt/β-catenin cascade exacerbates cardiac injury and adverse remodeling, whereas inhibition of β-catenin signaling could be cardioprotective.[17-19] In addition, Wnt/β-catenin signaling promotes cardiac fibrosis by inducing the transition of endothelial and epicardial cells to a mesenchymal state,[16,20,21] differentiation of fibroblasts into myofibroblasts, and collagen production.[22,23]

Although there is growing evidence regarding the role of both macrophages and Wnt signaling in infarct healing, the role of macrophage Wnt ligands in MI repair remains unknown. Therefore, we sought to determine whether macrophage Wnt ligands contribute toward infarct repair. Understanding the role of macrophage Wnt signaling in MI would not only expand our knowledge of infarct healing and

repair but could also define a new therapeutic target to improve infarct repair and regeneration.

Methods

Animals

To assess gene expression of the Wnt pathway in infarct macrophages and myocardium, we used 12-week-old BALB/c female mice (Harlan Laboratories, Jerusalem). In addition, we used female *Axin2-lacZ* (C57BL6) mice, which express the reporter gene *lacZ* under the control of Axin2, a universal Wnt target gene, and thus serve as reporters of β-catenin activity. To determine the effect of macrophage Wnt signaling on cardiac function and repair, we induced MI in a transgenic mouse previously described by Stefater et al.[24] In this study the Wnt ligand transporter *Wntless* (*Wls*), an essential element for Wnt ligand secretion,[25-27] was somatically deleted in macrophages, using the myeloid cre driver *cfms-icre*.[24,28] In this set of experiments both female and male mice were used to increase sample size in self-bred animals. To assess cre expression in macrophages, we used *cfms-icre* crossed with cre reporter *Rosa^{mT/mG}* mice (Jackson Laboratory, Bar Harbor, ME, stock no. 007576). C*fms-icre;Wls^{fl/fl}* and *Axin2-lacZ* mice were from the Lang laboratory (Cincinnati Children's Hospital Medical Center, Cincinnati, OH). Breeding and genotyping of *Axin2*,[11] *cfms-icre*[28] *Wls^{fl}*[27] and *Rosa^{mT/mG}*[29] were performed as previously described. The genotyping primers are listed in Table 1. All experimental procedures were approved by the Animal Care and Use Committee of Sheba Medical Center, Tel-Aviv University, which conforms to the policies of the American Heart Association and the *Guide for the Care and Use of Laboratory Animals* (Department of Health and Human Services, NIH Publication no. 85-23).

Experimental MI and Echocardiography Imaging

Mice (12-14 weeks old, n=110) were anesthetized by inhalation of 4% isoflurane. After anesthesia, mice were intubated and continued to receive 2% isoflurane by inhalation. The chest was opened by left thoracotomy via the fourth intercostal space, and the left coronary artery was permanently occluded with an intramural stitch, after which the chest was sutured closed.[3] C*fms-icre;Wls^{fl/fl}* and *Wls^{fl/fl}* mice are particularly vulnerable to MI, and mortality was up to 50% after MI surgery.[30]

Seven days before MI, and on days 1, 7, and 30 after MI, mice underwent transthoracic echocardiography imaging to assess cardiac function. The echocardiography imaging was performed using a commercially available echocardiography system (Vevo 2100, VisualSonics, Toronto, ON, Canada) equipped with a 32-MHz phased-array transducer (adapted for small animals). Echocardiography imaging and measurements were performed by a professional technician who was blinded to the experimental groups. Speckle-tracking-based strain imaging was performed and measured from 3 consecutive cardiac cycles taken at a frame rate of 300 frames per second, as previously described.[3]

PCR Array for Wnt Pathway Signaling

To evaluate the changes in Wnt pathway gene expression in MI compared with sham hearts, 500 ng of whole-heart total RNA from mice that underwent either MI or sham operations was analyzed using the Mouse WNT Signaling Pathway RT^2 Profiler PCR Array (SA Biosciences, Qiagen, Valencia, CA). To evaluate changes in gene expression of the Wnt pathway in infarct macrophages, compared with sham macrophages, 200 ng of total RNA isolated from macrophages was analyzed using the same PCR array. For data analysis, ΔΔCt was calculated. Data are presented as the average fold

Table 1. Genotyping Primers

Transcript	Forward Primer	Reverse Primer
Axin2 WT	5′-AAGCTGCGTCGGATACTTGAGA-3′	5′-AGTCCATCTTCATTCCGCCTAGC-3′
Axin2 Mut	5′-AAGCTGCGTCGGATACTTGAGA-3′	5′-TGGTAATGCTGCAGTGGCTTG-3′
Cfms-icre	5′-CTGGCTGTGAAGACCATC-3′	5′-CAGGGCCTTCTCCACACCAGC-3′
GAPDH	5′-TCGTCCCGTAGACAAAATGG-3′	5′-TTGAGGTCAATGAAGGGGTC-3′
IGF1	5′-TCATGTCGTCTTCACACCTCTTC-3′	5′-CCACACACGAACTGAAGAGCAT-3′
iNOS	5′-GTTCTCAGCCCAACAATACAAGA-3′	5′-GTGGACGGGTCGATGTCACA-3′
MMP12	5′-CATGAAGCGTGAGGATGTAGAC-3′	5′-TGGGCTAGTGTACCACCTTTG-3′
TGFβ1	5′-GGTTCATGTCATGGATGGTGC-3′	5′-TGACGTCACTGGAGTTGTACGG-3′
Wls recombined	5′-CTTCCCTGCTTCTTTAAGCGTC-3′	5′-CTCAGAACTCCCTTCTTGAAGC-3′
Wls fl	5′-AGGCTTCGAACGTAACTGACC-3′	5′-CTCAGAACTCCCTTCTTGAAGC-3′

change of log-normalized ratios of values from MI/sham hearts.

Real-Time PCR

Whole-heart total RNA was purified using EZ-RNA (Biological Industries, Beit HaEmek, Israel) according to the manufacturer's protocol. Genomic DNA contamination was removed using RQ1 RNase-free DNAse (Promega, Madison, WI). Isolated macrophage RNA was purified using the RNeasy Plus Microkit (Qiagen, Valencia, CA), and 200 ng of total macrophage RNA was reverse transcribed into cDNA using the High-Capacity cDNA Reverse Transcription Kit (Life Technologies, Carlsbad, CA). The expression of inducible nitric oxide synthase (iNOS), transforming growth factor β1 (TGFβ1), and insulin-like growth factor 1 (IGF1) was determined with SYBR Green PCR Master Mix (Life Technologies, Carlsbad, CA). Gene expression was normalized to the housekeeping gene glyceraldehyde 3-phosphate dehydrogenase (GAPDH). Data were analyzed using the ΔΔCt method with the aid of the StepOnePlus Software v2.2.2 (Applied Biosystems, Foster City, CA). Primers are listed in Table 1.

Cardiac Macrophage Isolation

To obtain cardiac macrophages, hearts were harvested 4 days after MI, and total heart cells were isolated using an enzymatic digestion mixture,[31] which was added to the heart for 3 15-minute cycles in a rotating water bath warmed to 37°C. Macrophages were purified based on plastic adherence, as previously described.[32] Briefly, cells were incubated for 2 hours at 37°C in humid air with 5% CO_2 on 6-well plates supplemented with RPMI (Biological Industries, Beit HaEmek, Israel) with 10% FBS and 1% penicillin-streptomycin (Biological Industries, Beit HaEmek, Israel). Then, nonadherent cells were washed, and, to further ensure macrophage enrichment, a 3-minute trypsin-EDTA treatment was added to the remaining cells.[3] The trypsin was then blocked with fresh medium and washed, and the intact adherent cells were considered cardiac macrophages. To determine purification efficiency, the cells were stained with the macrophage marker F4/80 and displayed >90% positive staining for F4/80 in culture. Next, cardiac macrophages were either immediately lysed for RNA purification or grown for 24 hours for conditioned media collection.

Flow Cytometry

To assess the effect of *Wntless* deletion on macrophage polarization after MI, the immune phenotype of isolated cells from hearts of *cfms-icre;Wls^fl/fl* and *Wls^fl/fl*, 4 days after MI, was analyzed by flow cytometry, using the following fluorescent antimouse antibodies: CD206, CD86, CD11b, and F4/80 (BioLegend, San Diego, CA). Labeled cells (0.5×10^6) from each sample were acquired and analyzed using FACS Calibur Cytofluorimeter (BD Biosciences, San Jose, CA) and Flowjo software (Tree Star, Ashland, OR), as previously described.[3]

Cytokine Array

To determine the levels of cytokine secretion from macrophages, we cultured whole heart cells at a concentration of 1.5×10^6 per well in a 48-well plate and purified macrophages 2 hours later using the plastic adherence protocol described above. Macrophages were cultured for 24 hours, and culture media was collected and stored at −80°C until use. Inflammatory cytokine levels were analyzed using a custom (10-plex) Bio-Plex Pro™ Mouse Cytokine Assay (Bio-Rad, Hercules, CA) according to the manufacturer's protocol. All samples were run in duplicate wells.

Angiogenic Tube Formation Assay

To determine the angiogenic properties of macrophages from *cfms-icre;Wls^fl/fl* and *Wls^fl/fl* mice, human umbilical vein endothelial cells (HUVECs) (Promocell, Heidelberg, Germany) were seeded in a concentration of 3×10^4 cells/well onto 96-well plates coated with 50 μL of matrigel matrix (Corning, Corning, NY) and allowed to attach. Then, 100 μL of each of the macrophage's conditioned medium samples was added in triplicate and incubated for 6 hours, after which microscopic images were taken (1 image per well at ×10 magnification). The number and structure of the tubes were evaluated by an independent observer who was blinded to the different groups. Results from the triplicate wells were averaged and expressed as the mean number of tubes per well.

Histological Analysis of Mouse Hearts After MI

Hearts were harvested for histological examination on days 4, 7, and 30 after MI (after last echocardiography). To fixate the heart, mice underwent whole-body perfusion with 4% buffered formaldehyde (Biolab, Jerusalem, Israel). Hearts were then harvested, sectioned into 4 transverse slices parallel to the atrioventricular ring, fixed, and embedded in paraffin blocks. Each block was sectioned into 5-μm slices. To examine Wnt signaling activity and macrophage accumulation, sections were stained for β-catenin and MAC-3 (BD Biosciences, San Jose, CA). In immunofluorescent images, heart sections were stained with β-catenin (BD Biosciences, San Jose, CA) and Alexa Fluor 647 secondary antibody (Cell Signaling Technology, Danvers, MA), and images (×40 oil) were captured with an LSM 700 confocal microscope operated by Zen 2012
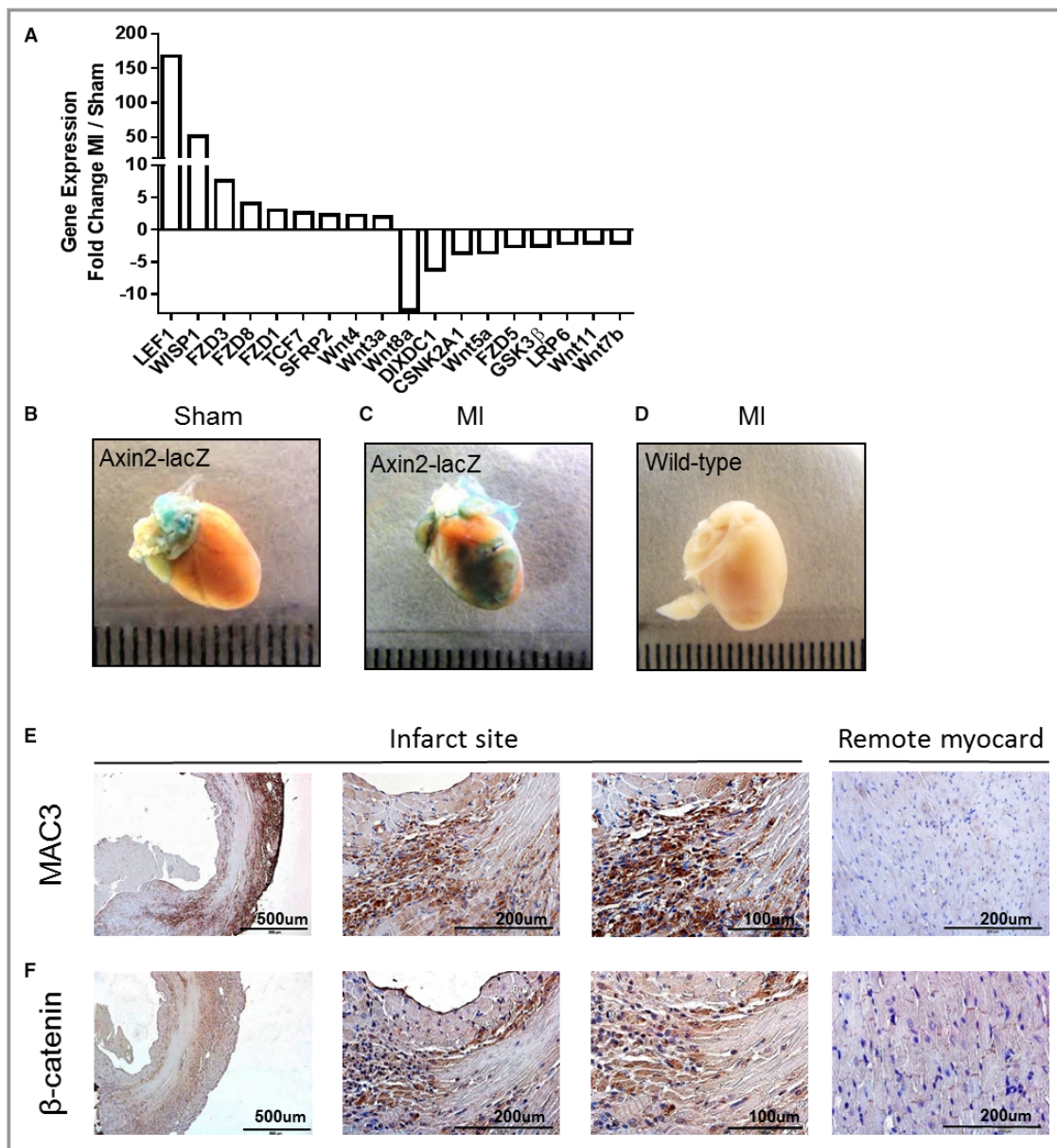
Figure 1. Changes in Wnt signaling after MI, whole-heart analysis. A, A mouse PCR array for the Wnt signaling pathway was performed on mouse hearts after either MI or sham operations. The highly up- or downregulated genes (>2- or < −2-fold change) are displayed as fold change between MI and sham hearts (n=2 in each group). B, Canonical Wnt signaling is evident (positive β-gal staining) in the large vessels at the base of the heart under normal sham conditions. C, Enhanced β-gal staining, indicating canonical Wnt signaling, at the infarct site after MI. D, WT mice do not display β-gal staining after MI and the same staining procedure for lacZ detection. E and F, MAC3 and β-catenin staining for histological assessment of macrophages and Wnt signaling in the heart, 4 days after MI. High amounts of infiltrating macrophages (E) and Wnt signaling activity (F) are evident near the infarct area (×4, ×40, and ×60 magnifications). Remote uninjured myocardium shows weak staining for macrophages (E) and β-catenin (F) limited to adherens junctions. G, Section from day 4 infarct zone of *cfms-icre × Rosa*$^{mT/mG}$ reporter mice. Infarct macrophages are labeled by GFP (green) and are distinct from β-catenin (red) activity in adjacent infarct cells, ×40 magnification. CSNK2A1 indicates casein kinase 2, α1 polypeptide; FZD, frizzled class receptor; GSK3β, glycogen synthase kinase 3β; LEF1, lymphoid enhancer-binding factor 1; MI, myocardial infarction; PCR, polymerase chain reaction; SFRP2, secreted frizzled-related protein 2; TCF7, transcription factor 7; WISP1, Wnt1-inducible signaling pathway protein 1; WT, wild-type.

software (ZEISS, Oberkochen, Germany). Masson trichrome (Sigma-Aldrich, Rehovot, Israel) was used to detect fibrosis and scar formation at the midsection of the heart, and scar area was measured using planimetry software (Sigma Scan Pro version 5, San Jose, CA). To assess vessel density, sections were stained for CD31 (Santa Cruz Biotechnology,
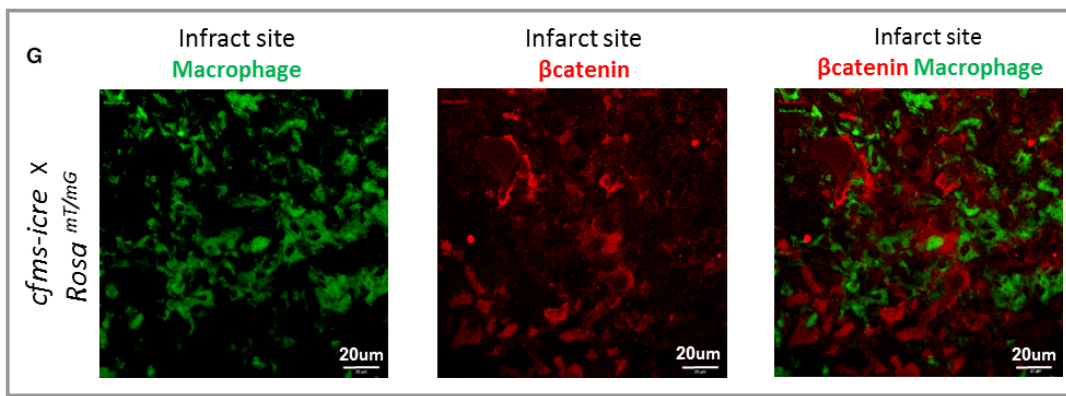
Figure 1. Continued

Dallas, TX) and vessel density (mean arteriole and capillary number/mm^2) was measured from 3 adjacent fields near the infarct border of each section, at ×40 magnification. β-Gal activity in *Axin2-lacZ* reporter mice was assessed using the β-Galactosidase Reporter Gene Staining Kit (Sigma-Aldrich, Rehovot, Israel) according to the manufacturer's protocol.

Statistical Analysis

Statistical analysis was performed with GraphPad Prism version 6.00 for Windows (GraphPad Software, La Jolla, CA, www.gra phpad.com). All variables are expressed as mean±SEM. Normality was tested with the Kolmogorov-Smirnov test. Differences between groups were assessed by 2-tail unpaired t tests. The nonparametric Mann-Whitney test was used if data were not normally distributed. To test the hypothesis that changes in measures of left ventricular (LV) remodeling and function over time vary among the experimental groups, we used general linear model 2-way repeated-measures ANOVA. Echocardiography measures of LV remodeling and function at baseline, day 1, day 7, and day 30 after MI were analyzed, and the Bonferroni correction was used to assess the significance of predefined comparisons at specific time points.

All authors had full access to and take full responsibility for the integrity of the data. All authors have read and agree to the manuscript as written.

Results

Changes in Wnt Pathway Gene Expression After MI

To determine whether the Wnt pathway is involved in healing and repair after MI, we performed a comprehensive, real-time PCR array, which analyzes genes associated with the Wnt signaling pathway on mouse hearts, 4 days after either MI or sham operations. Several key genes of the Wnt pathway were highly expressed after MI, compared with sham-operated mice (Figure 1A). Notably, lymphoid enhancer-binding factor 1 (LEF-1), a transcription factor of the Wnt/β-catenin pathway, was highly upregulated after MI (a 168-fold change), followed by WNT1-inducible signaling pathway protein 1 (WISP1) (a 52-fold change), a molecule that was found to stimulate fibroblast proliferation, cardiomyocyte hypertrophy, and extra-cellular matrix (ECM) expression in vitro.[33] MI was also associated with a downregulation of several Wnt pathway genes, specifically the Wnt ligands Wnt8a, Wnt5a, Wnt11, and Wnt7b (12.5-, 3.6-, 2-, and 2-fold changes, respectively) and the canonical Wnt pathway inhibitors—casein kinase 2 α1 polypeptide (CSNK2A1), glycogen synthase kinase 3β (GSK3B), and Wnt inhibitory factor 1 (WIF1) (3.6-, 2.5-, and 2.2-fold changes, respectively) (Figure 1A). A comprehensive list of all Wnt pathway genes differently expressed in MI and sham hearts is presented in Table 2. Together, our results show that MI triggers a significant change in the Wnt cascade, suggesting its involvement in cardiac repair after MI.

Accumulation of Macrophages and Activation of Wnt/β-Catenin Signaling After MI

We next induced MI in *Axin2-lacZ* Wnt pathway reporter mice. These mice contain the β-galactosidase gene under the control of Axin2, an important Wnt target gene, which is induced by canonical Wnt signaling and therefore serves as a reporter for canonical Wnt activity.[34] Notably, high β-gal activity (indicating active Wnt signaling) was observed at the infarct zone of the reporter mice but not in wild-type (WT) MI mice or sham-operated reporters (Figure 1B through 1D). To determine the correlation between active Wnt signaling and the inflammatory response after MI, we stained consecutive histological sections of hearts 4 days after MI (when the peak of macrophage recruitment occurs)[3] for the macrophage marker-MAC3 and for β-catenin, which is the key downstream effector of the canonical Wnt pathway. We observed high

Table 2. List of Wnt Pathway Genes Upregulated or Downregulated in the Infarcted Heart Compared With Sham Hearts

| Gene Name	Full Name	Function	Fold Change
Upregulated genes of the Wnt pathway in MI vs Sham hearts			
LEF1	Lymphoid enhancer-binding factor 1	Transcription factor. Activates transcription of target genes in the presence of CTNNB1 and EP300	168.8
WISP1	WNT1-inducible signaling pathway protein 1	Belongs to the connective tissue growth factor family. Expressed at high levels in fibroblast cells, and overexpressed in colon tumors. Associated with cell survival	51.9
Fosl1	FOS-like antigen 1	Forms the transcription factor complex AP-1 with proteins of the JUN family. Implicated as regulator of cell proliferation, differentiation, and transformation	12.4
FZD3	Frizzled class receptor 3	Receptor for Wnt proteins	7.6
Fzd8	Frizzled class receptor 8	Receptor for Wnt proteins	4.1
Wnt9a	Wingless-type MMTV integration site family, member 9A	Ligand for members of the frizzled family of 7-transmembrane receptors	3.7
Fzd1	Frizzled class receptor 1	Receptor for Wnt proteins	3.1
TCF7	Transcription factor 7	Binds an enhancer element and activates the CD3E gene and also may repress the CTNNB1 and TCF7L2 genes through a feedback mechanism	2.6
SFRP2	Secreted frizzled-related protein 2	Modulates Wnt signaling through direct interaction with Wnts	2.3
Wnt4	Wingless-type MMTV integration site family, member 4	Ligand for members of the frizzled family of 7-transmembrane receptors. Probable developmental protein	2.2
Wnt3a	Wingless-type MMTV integration site family, member 3A	Ligand for members of the frizzled family of 7-transmembrane receptors	2.0
Downregulated genes of the Wnt pathway in MI vs sham hearts			
Wnt8a	Wingless-type MMTV integration site family 8A	Ligand for members of the frizzled family of 7-transmembrane receptors	−12.5
Dixdc1	DIX domain containing 1	Positive effector of the Wnt signaling pathway; activates WNT3A signaling via DVL2	−6.2
Wnt5a	Wingless-type MMTV integration site family 5A	Ligand for members of the frizzled family of 7-transmembrane receptors	−3.6
Csnk2a1	Casein kinase 2, α1 polypeptide	Regulates Wnt signaling by phosphorylating CTNNB1 and the transcription factor LEF1	−3.6
Btrc	β-Transducin repeat containing E3 ubiquitin protein ligase	Mediates the ubiquitination of CTNNB1 and participates in Wnt signaling	−3.0
Daam1	Disheveled associated activator of morphogenesis 1	Binds to disheveled (Dvl) and Rho, and mediates Wnt-induced Dvl-Rho complex formation. Regulates cell growth	−2.9
Fzd5	Frizzled class receptor 5	Receptor for Wnt proteins	−2.6
Frat1	Frequently rearranged in advanced T-cell lymphomas	Belongs to the GSK-3-binding protein family. Inhibits GSK-3-mediated phosphorylation of β-catenin and positively regulates the Wnt signaling pathway	−2.5
Gsk3b	Glycogen synthase kinase 3β	Forms a multimeric complex with APC, AXIN1, and CTNNB1/β-catenin and phosphorylates the N-terminus of CTNNB1 leading to its degradation	−2.5
Nlk	Nemo-like kinase	Positive effector of the noncanonical Wnt signaling pathway, acting downstream of WNT5A	−2.5
Wif1	WNT inhibitory factor 1	Binds to WNT proteins and inhibits their activities	−2.2
Pygo1	Pygopus family PHD finger 1	Involved in signal transduction through the Wnt pathway	−2.2
Prickle 1	Prickle homologue 1	Involved in the planar cell polarity pathway. Negative regulator of the Wnt/β-catenin signaling pathway	−2.2
Csnk1a1	Casein kinase 1, α1	Phosphorylates CTNNB1 as part of its degradation process	−2.1
LRP6	Low-density lipoprotein receptor-related protein 6	A receptor or, with frizzled, a coreceptor for Wnt; thereby transmits the canonical Wnt/β-catenin signaling cascade	−2.1
Wnt11	Wingless-type MMTV integration site family 11	Ligand for members of the frizzled family of 7-transmembrane receptors	−2.0
Wnt7b	Wingless-type MMTV integration site family 7b	Ligand for members of the frizzled family of 7-transmembrane receptors	−2.0
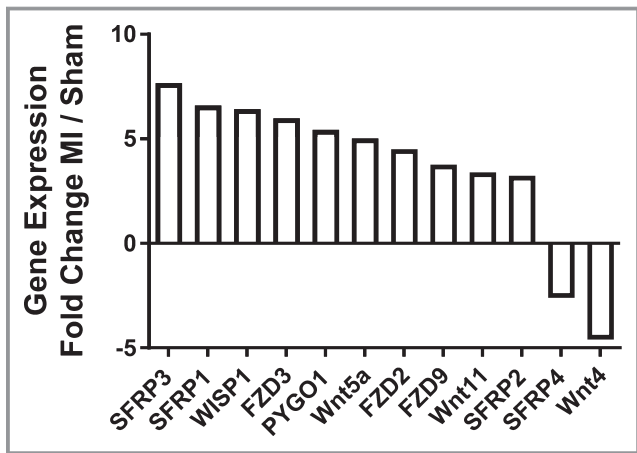
Figure 2. Macrophages express specific components of the Wnt signaling pathway after MI. A mouse Wnt Pathway PCR array was performed on isolated macrophages, 4 days after either MI or sham operation. The highly up- or downregulated genes (>2- or <−2-fold change) are displayed as fold change between macrophages from MI and sham hearts. FZD indicates frizzled class receptor; MI, myocardial infarction; PCR, polymerase chain reaction; PYGO1, pygopus family PHD finger 1; SFRP, secreted frizzled-related protein; WISP1, Wnt1-inducible signaling pathway protein 1.

numbers of macrophages surrounding the infarct site 4 days after MI, as opposed to the remote myocardium (Figure 1E). At the same time point, β-catenin was detected in the infarct border zone, whereas in the uninjured remote myocardium, β-catenin was visible at adherens junctions only, where it

assumes a physiological role of cell-cell adhesion (Figure 1F).[35,36] Heart sections of *cfms-icre* × *Rosa^{mT/mG}* reporter mice, in which macrophages express GFP, were stained in order to further localize the source of β-catenin in the infarcted myocardium. Four days after MI, the highest response to canonical Wnt signaling was in infarct cells other than macrophages, most probably smooth muscle cells, endothelial cells, fibroblasts, and myofibroblasts (Figure 1G). Together, marked Wnt activity at 4 to 7 days after MI and its localization to the site of macrophage accumulation near the infarct, suggest the involvement of Wnt signaling in post-MI inflammation and repair.

Expression of Wnt Pathway Components by Infarct Macrophages

Having found high Wnt activity at the site of macrophage accumulation after MI, we aimed to test whether infarct macrophages are a source of Wnt ligands in the injured heart. We isolated macrophages from the infarcted heart, as previously described,[3] and analyzed the levels of mRNAs encoding ligands, receptors, and other components of the Wnt pathway using a Wnt pathway PCR array. The results of the array revealed that infarct macrophages have a distinct transcriptional profile of the Wnt signaling pathway after MI (Figure 2). As in the whole-heart expression analysis, infarct macrophages displayed increased levels of WISP1, FZD3, and SFRP2. Distinctly, and in contrast to the myocardial Wnt
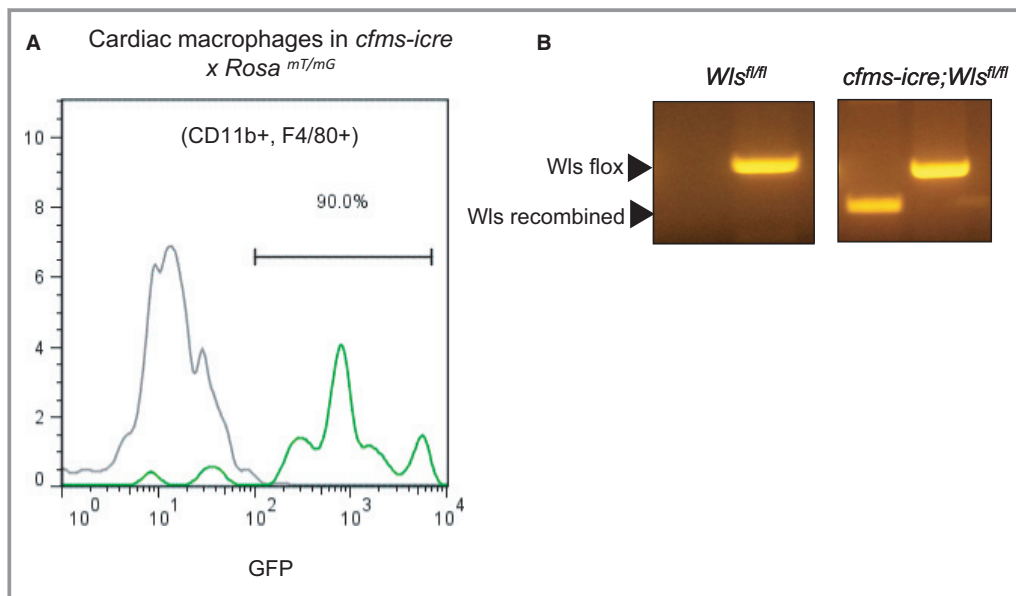
Figure 3. Expression of *cfms-icre* in cardiac macrophages and genotyping for *Wls^{fl}*. A, Flow cytometry analysis of GFP expression in cre reporter mice *Rosa^{mT/mG}* crossed with *cfms-icre* compared with controls (*Rosa^{mT/mG}*), demonstrating the activation of the *cfms-icre* transgene (GFP+) in cardiac macrophages (CD11b+ and F4/80+). B, Genotyping for the *Wls^{fl}* allele shows the presence of the recombined *Wls^{fl}* allele only in *cfms-icre* mice.
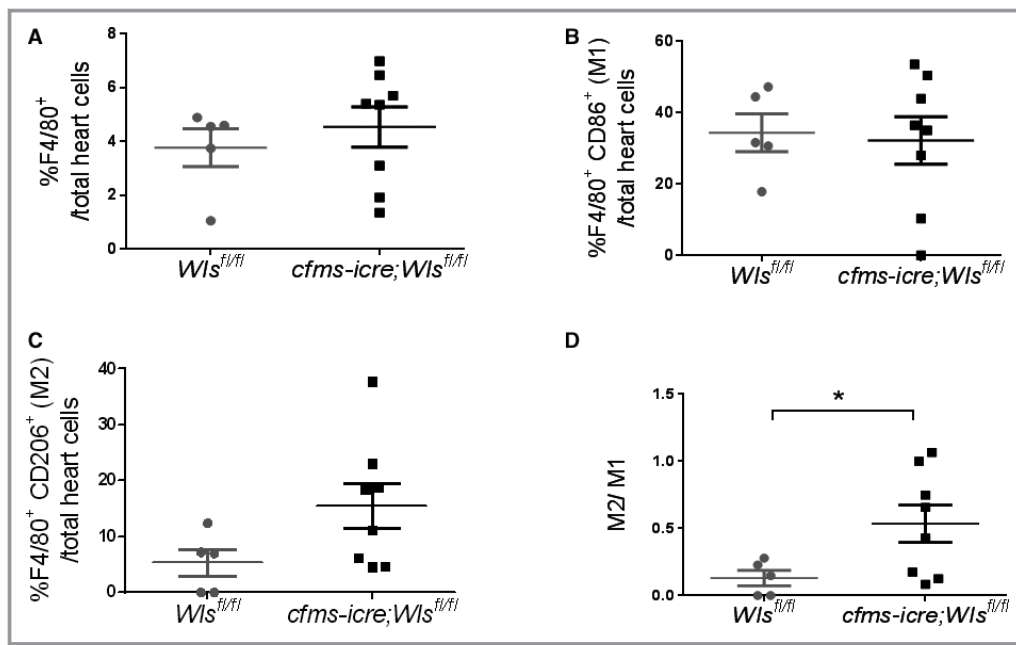
Figure 4. *Wls* deficiency in cardiac macrophages increases cardiac M2 to M1 ratio 4 days after MI. Flow cytometry analysis of mouse hearts for macrophage (F4/80), M1 (CD86) and M2 (CD206) percentages, 4 days after MI. A and B, No difference in total macrophage (A) or M1 (B) percentage after MI between *cfms-icre;Wls*^{fl/fl} and *Wls*^{fl/fl} mice. C, A shift toward M2 in *cfms-icre;Wls*^{fl/fl} mice. D, Increased M2 to M1 ratio in c*fms-icre;Wls*^{fl/fl} hearts after MI (n=8 in *cfms-icre;Wls*^{fl/fl}, n=5 in *Wls*^{fl/fl} group). Results are presented as mean±SEM. Statistical analysis: 2-tailed unpaired Student t test. *$P<0.05$ vs *Wls*^{fl/fl}. *Cfms* indicates colony-stimulating factor 1 receptor; MI, myocardial infarction; *Wls, Wntless*.

expression profile, infarct macrophages exhibited an increase in the noncanonical Wnt ligands Wnt5a and Wnt11 (5- and 3-fold changes, respectively) compared with macrophages from sham-operated hearts. Infarct macrophages also demonstrated increased levels of the frizzled receptors FZD3, FZD2, and FZD9 and Wnt pathway modulators such as SFRP3, SFRP1, and PYGO1. The downregulated Wnt pathway genes in infarct macrophages were SFRP4 and WNT4. These results suggest that macrophages mediate a Wnt pathway response in the heart after ischemic injury and that infarct macrophages selectively upregulate the noncanonical Wnt pathway in response to cardiac injury.

Characterization of *Wls*-Deficient Macrophages

To determine the effect of macrophage Wnt signaling on post-MI repair, we induced MI in *cfms-icre;Wls*^{fl/fl} mice, previously described by Stefater et al.[24] These mice lack the essential Wnt ligand transporter *Wls* in macrophages, using the myeloid cre driver *cfms-icre,* and, therefore, are unable to secrete Wnts from macrophages.[24] A cre reporter mouse, *Rosa*[mT/mG] crossed with *cfms-icre* was used to confirm the presence of the transgene in cardiac macrophages (Figure 3). To phenotypically characterize *Wls*-deficient macrophages 4 days after MI, we used flow cytometry and the macrophage markers F4/

80, CD206 (an M2 marker),[3,5,37] and CD86 (an M1 marker).[3,37] We favored these M1 and M2 markers based on our previous experience,[3,37] that of others,[5,38] and the potential to apply these markers in human macrophage studies.[39] Compared with controls, macrophage *Wls* deficiency did not affect the overall percentage of macrophages (Figure 4A) or the CD86^{+} macrophage subtype in the infarcted heart (Figure 4B). However, the percentage of the CD206-positive macrophage subset was higher, and there was an increase in the ratio of M2 to M1 in c*fms-icre;Wls*^{fl/fl} hearts compared with controls (Figure 4C and 4D). To define the reparative properties of the macrophages, we isolated infarct macrophages from *cfms-icre;Wls*^{fl/fl} and *Wls*^{fl/fl} mice 4 days post-MI and collected their conditioned media after 24 hours in culture. Macrophage-conditioned media were next analyzed using a cytokine array to assess the levels of different inflammatory cytokines. Interestingly, macrophages with loss of Wnt secretion produced greater amounts of the proangiogenic vascular endothelial growth factor (VEGF), interleukin-6 (IL-6), and interleukin-2 (IL-2) (Figure 5A). Furthermore, they displayed a marked reduction in the secretion of the proinflammatory interleukin-1α (IL-1α) and the profibrotic basic fibroblast growth factor (bFGF) and interleukin-13 (IL-13), compared with control macrophages (Figure 5A). To validate the proangiogenic properties of *Wls*-deficient
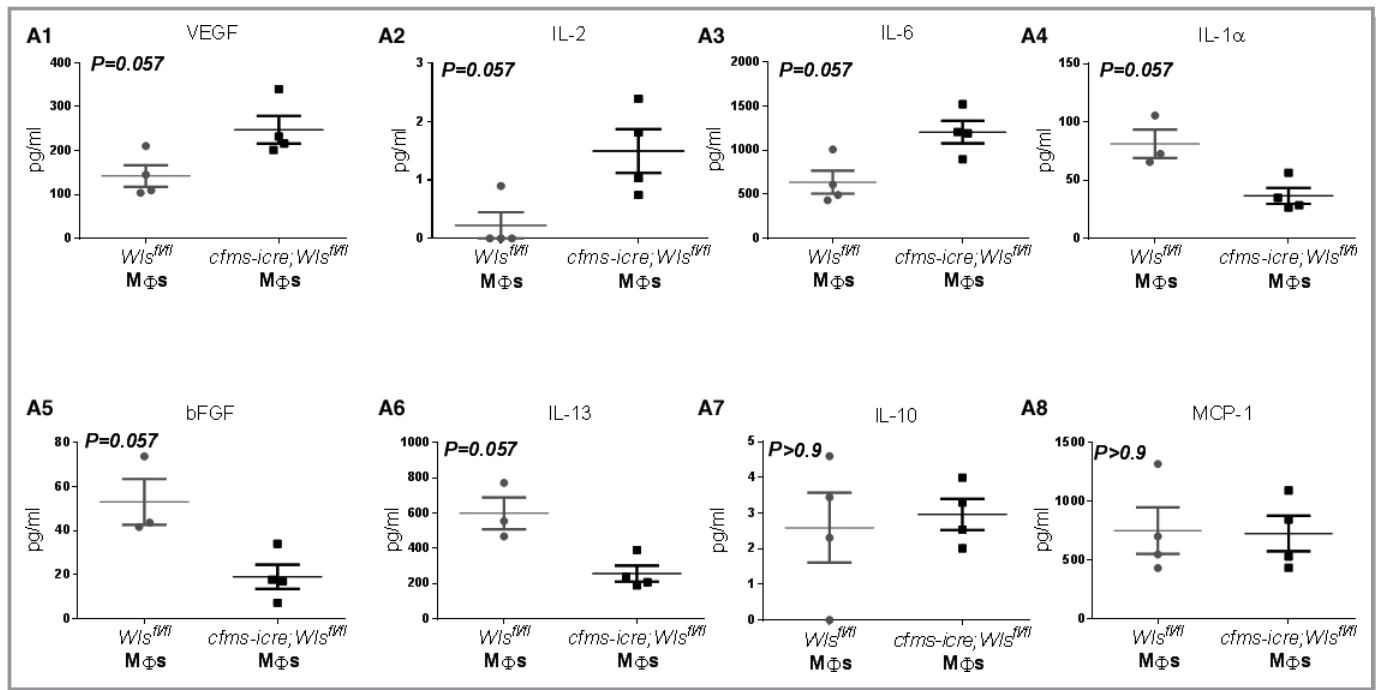
Figure 5. *Wls*-deficient infarct macrophages show increased reparative and proangiogenic properties after MI. A1 through A8, Infarct macrophages with *Wls* deletion display a proangiogenic and antifibrotic cytokine secretion profile. A Magnetic Mouse Bioplex screening assay was performed using conditioned media from *Wls*-deficient and control infarct macrophages isolated 4 days after MI. *Wls*-deficient macrophages secreted higher levels of the proangiogenic VEGF (A1), IL-2 (A2), and IL-6 (A3) cytokines (n=4 in each group) and lower levels of IL-1α (A4), bFGF (A5), and IL-13 (A6) compared with controls (n=4 in *cfms-icre;Wls^{fl/fl}* and n=3 in the control group). There was no difference in the levels of IL-10 (A7) or MCP-1 (A8) between the conditioned media of *Wls*-deficient and control macrophages. To support the secretome data, the angiogenic capacity of conditioned media from macrophages lacking *Wls* was determined by HUVEC tube formation assay. B1, *Wls*-deficient macrophages are proangiogenic and induced 31% more HUVEC tube formations compared with controls. B2 and B3, Representative images of the matrigel tube formation assay, which show an increased number of vessel-like formations in the *Wls*-deficient macrophage-conditioned medium group, ×4 magnification (n=8 in *cfms-icre;Wls^{fl/fl}* and n=7 in the control group). C1 through C3, qPCR analysis of reparative gene expression in isolated cardiac macrophages from *cfms-icre;Wls^{fl/fl}* and *Wls^{fl/fl}* 4 days after MI. *Wls*-deficient macrophages express higher levels of iNOS (C1), TGFβ1 (C2), and IGF1 (C3) compared with control macrophages (n=5 in each group). The relative expression is normalized to GAPDH levels. All results are presented as mean±SEM. Statistical analysis: differences between groups were assessed by 2-tail unpaired t tests. The nonparametric Mann-Whitney test was used if data were not normally distributed. bFGF indicates basic fibroblast growth factor; *cfms*, colony-stimulating factor 1 receptor; IGF-1, insulin-like growth factor 1; IL, interleukin; iNOS, inducible nitric oxide synthase; MI, myocardial infarction; Mφ, macrophage; TGFβ1, transforming growth factor β1; VEGF, vascular endothelial growth factor; *Wls*, *Wntless*.

macrophages, we performed a HUVEC tube formation assay using the macrophage-conditioned media from *Wls*-deficient and control infarct macrophages. Significantly, the conditioned media of macrophages lacking *Wls* increased tube formation compared with those of control macrophages (Figure 5B).

Finally, we assessed expression of several key genes associated with macrophage polarization and function in the infarct macrophages. Significantly, *Wls*-deficient macrophages upregulated the expression of inducible nitric oxide synthase (iNOS), transforming growth factor-β1 (TGFβ1), and insulin-like growth factor 1 (IGF1) compared with control macrophages (Figure 5C). Together, *Wls*-deficient macrophages generated a unique subset of infarct macrophages characterized by an M2-like phenotype with angiogenic, antifibrotic, and reparative properties.

Deficiency of Macrophage Wnt Signaling Improves Cardiac Repair

Next, to assess whether loss of macrophage Wnt secretion affects infarct healing and repair, MI was induced in *cfms-icre;Wls^{fl/fl}* mice and their littermate controls (*Wls^{fl/fl}*). Cardiac function and remodeling were assessed before injury (baseline) and on days 1, 7, and 30 after MI by 2D echocardiography. Although there was no significant difference in baseline cardiac function between controls and *cfms-icre;Wls^{fl/fl}* mice, cardiac contractility was significantly improved in *cfms-icre;Wls^{fl/fl}* mice 30 days after MI (Figure 6A and 6B). Particularly, the typical post-MI deterioration in LV ejection fraction was attenuated by 2.75-fold in the *cfms-icre;Wls^{fl/fl}* group at 30 days after MI (Figure 6C). Furthermore, cardiac remodeling, assessed by LV posterior wall thickness and LV
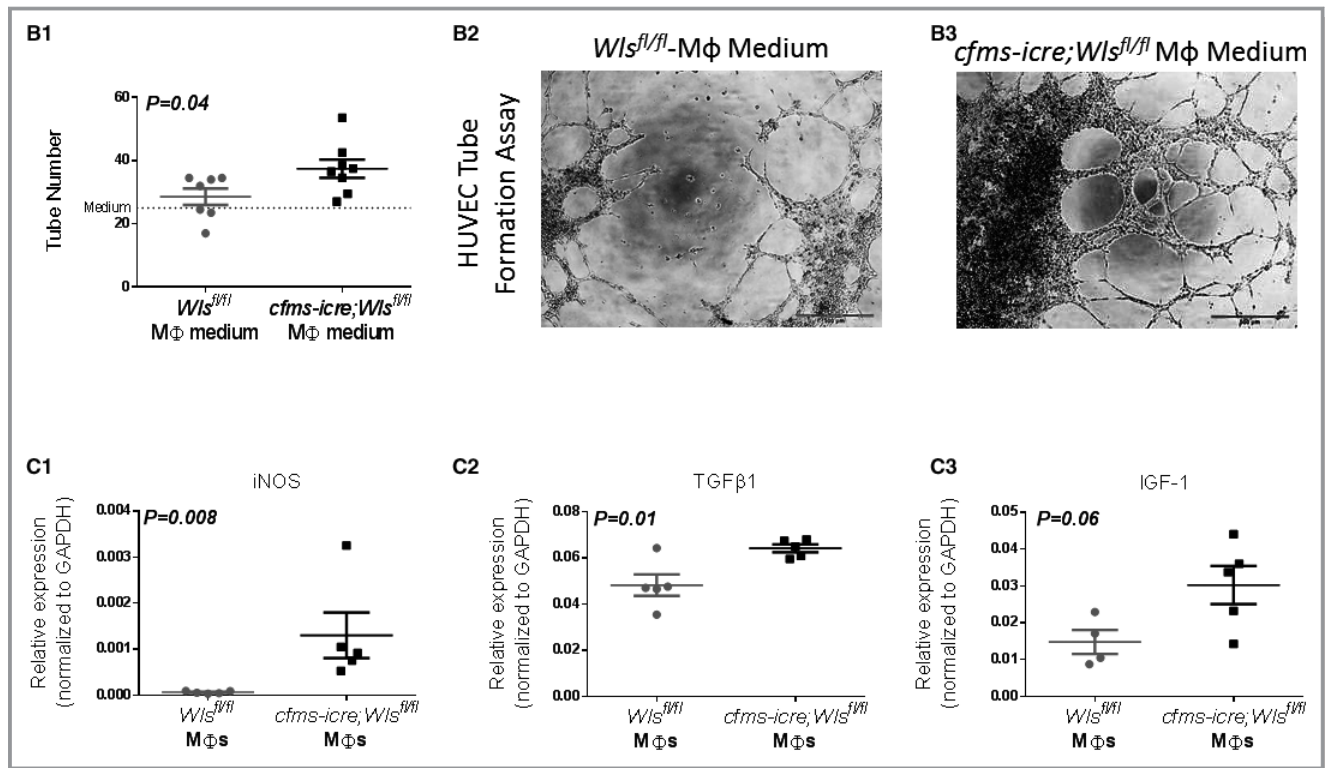
Figure 5. Continued

end-systolic area, was improved in *cfms-icre;Wls*^{fl/fl} mice 30 days after MI (Figure 6D and 6E). LV end-diastolic area was similar in *cfms-icre;Wls*^{fl/fl} and control mice (Figure 6F). The full echocardiography variables analyzed are listed in Table 3. Finally, subgroup analysis demonstrated that the favorable effect of macrophage *Wls* deletion was preserved in both the male and female mice when analyzed separately (Figure 7).

To confirm the echocardiography findings, we analyzed global and regional myocardial function after MI using the highly sensitive LV speckle-tracking-based strain analysis. The results from the strain analysis showed that *Wls* deletion in macrophages was associated with improved regional function of the anterior apex, apical, and midposterior segments, which contributed to an overall improved global strain in both longitudinal and radial strain imaging (Figure 8).

Macrophage Wnt ligands have been shown to regulate angiogenesis in various models.[24,40] Having shown that *Wls*-deficient macrophages are proangiogenic (Figure 5), we aimed to determine whether *Wls* deletion in macrophages also affects myocardial angiogenesis after MI. To do so we obtained histological sections of mouse hearts 30 days after MI, when myocardial healing has largely been completed and is characterized by a fibrotic scar and newly formed vessels. Angiogenesis was measured by assessing the number of small

(<20 μm in diameter) CD31-positive blood vessels near the infarcted area in *cfms-icre;Wls*^{fl/fl} and *Wls*^{fl/fl} hearts. Notably, the number of small vessels was 66% higher in mice lacking macrophage Wnts compared with controls (164 ± 11.5 vs 98.8 ± 10.6, respectively; Figure 9).

Wnt signaling has also been implicated in cardiac fibrosis.[21] Thus, we evaluated scar thickness and area by Masson trichrome staining 30 days post-MI. However, infarct size and scar thickness in control and *cfms-icre; Wls*^{fl/fl} groups were similar (Table 4), suggesting that the improved myocardial function and repair observed in mice lacking macrophage Wnts were independent of infarct size or fibrosis but rather were mediated by enhanced angiogenesis and the reparative M2-like paracrine profile of *Wls*-deficient macrophages.

Discussion

Our results suggest, for the first time, that inhibiting Wnt secretion in macrophages improves cardiac healing and function after MI. Deletion of the *Wls* gene in myeloid cells results in a shift toward M2-like macrophages with anti-inflammatory, reparative, and angiogenic properties, increased angiogenesis at the infarct border zone, and improved LV function and remodeling 1 month after MI. Although there are studies that have demonstrated improved
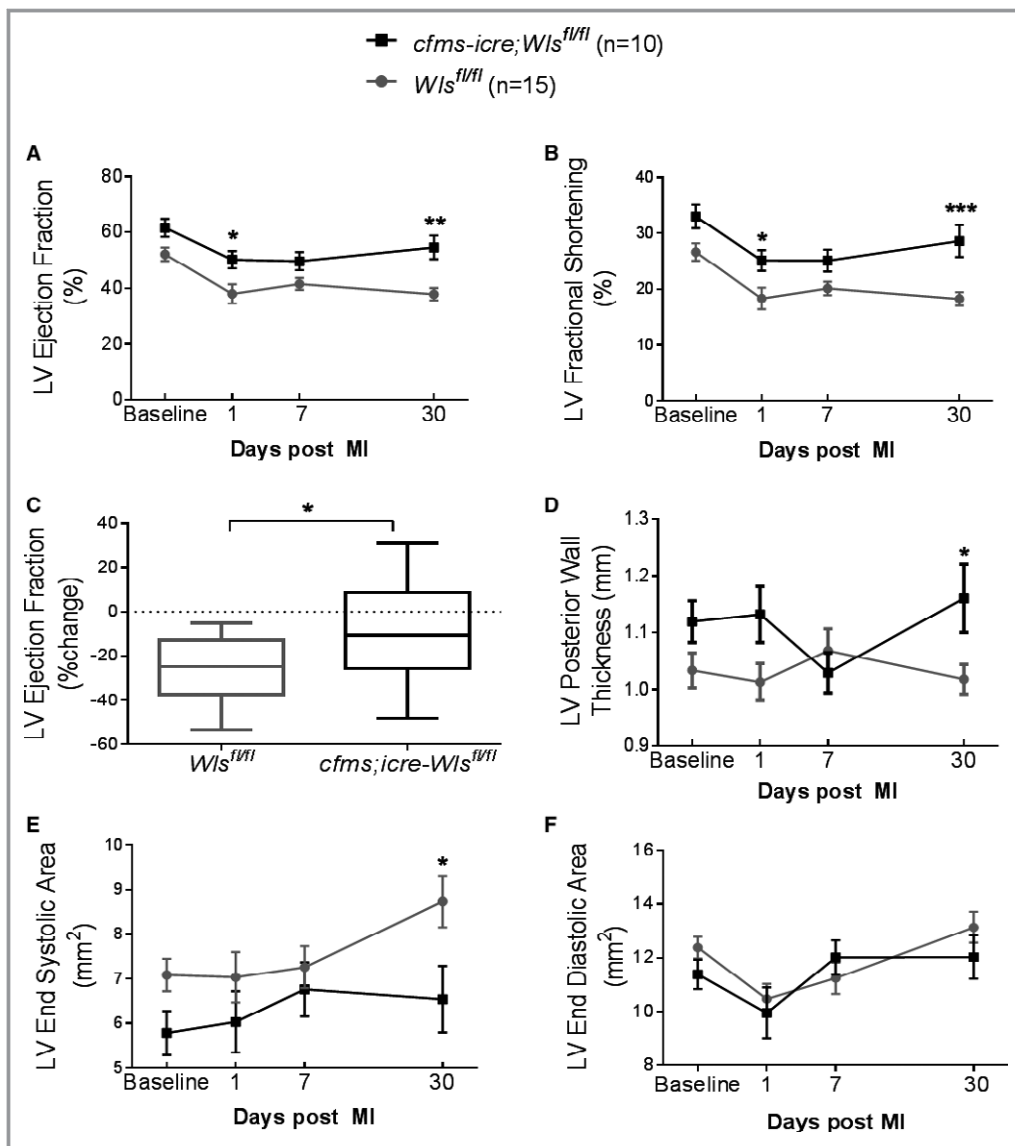
Figure 6. *Wls* deficiency in macrophages improves cardiac function and remodeling 30 days after MI. MI was induced in *cfms-icre;Wls^fl/fl* and controls, and cardiac remodeling and function were determined by echocardiography measurements at 4 different time points. *Wls* deletion in macrophages improved heart function as determined by ejection fraction (A), fractional shortening (B), and change in ejection fraction (C). LV remodeling was less adverse in *cfms-icre;Wls ^fl/fl* animals, indicated by preserved LV wall thickness during systole (D) and smaller LV end-systolic volume (E). LV end diastolic area (F) was not significantly reduced compared with *Wls^fl/fl* mice. Black line, *cfms-icre;Wls^fl/fl* (n=10); gray line, *Wls^fl/fl* (n=15). All results are presented as mean±SEM. Statistical analysis: 2-way repeated-measures analysis of variance with Bonferroni posttest. *$P<0.05$, **$P<0.01$, ***$P<0.001$ vs *Wls^fl/fl*. *Cfms* indicates colony-stimulating factor 1 receptor; LV, left ventricle; MI, myocardial infarction; *Wls*, Wntless.

myocardial vascularization, healing, and function from inhibiting the Wnt signaling pathway after MI,[18,19,41] it is unclear which cardiac cell is responsible for such protection. We have demonstrated that specific targeting of the Wnt signaling pathway in macrophages is sufficient to improve cardiac remodeling and function after MI. Therefore, our work highlights the importance of macrophages in mediating the Wnt response after MI.

Importantly, our study demonstrates that infarct macrophages are a source of noncanonical Wnt ligands after MI. It should be noted that when we analyzed the expression profile of Wnt signaling in the whole heart, we noticed an upregulation of key genes of the pathway, including canonical Wnt genes and histologically high β-catenin levels, indicating active canonical Wnt signaling. Previous reports have shown that MI activates canonical Wnt signaling in endothelial cells,

Table 3. LV Parameters Analyzed by 2D Echocardiography in *cfms-icre;Wls*$^{fl/fl}$ and *Wls*$^{fl/fl}$ Mice at Baseline and Days 1, 7, and 30 After MI

	Days After MI	Wls$^{fl/fl}$ (n=15)	cfms-icre;Wls$^{fl/fl}$ (n=10)	P (Repeated-Measures ANOVA)		
				Wls−/− Effect	Time Effect	Interaction
Ejection fraction, %	Baseline	52.14±2.39	61.65±3.22	0.0011	<0.0001	0.2944
	1*	38.05±3.43	50.26±3.16			
	7	41.58±2.16	49.66±3.27			
	30‡	37.88±2.23	54.64±4.23			
LV diastolic area, mm^2	Baseline	12.38±0.41	11.38±0.54	0.4975	<0.0001	0.2069
	1	10.47±0.56	9.94±0.95			
	7	11.24±0.59	12.01±0.64			
	30	13.14±0.57	12.02±0.80			
LV systolic area, mm^2	Baseline	7.08±0.36	5.78±0.49	0.0547	0.0249	0.2552
	1	7.03±0.56	6.03±0.69			
	7	7.26±0.47	6.76±0.60			
	30*	8.72±0.57	6.54±0.74			
Fractional shortening, %	Baseline	26.63±1.56	33.01±2.11	0.0007	<0.0001	0.3361
	1*	18.36±1.93	25.15±1.88			
	7	20.14±1.19	25.11±1.97			
	30‡	18.28±1.21	28.63±2.88			
Posterior wall thickness, diastole, mm	Baseline	0.75±0.01	0.79±0.02	0.5700	0.1818	0.1680
	1	0.78±0.02	0.82±0.04			
	7	0.81±0.02	0.76±0.01			
	30	0.81±0.01	0.82±0.02			
Posterior wall thickness, systole, mm	Baseline	1.03±0.03	1.11±0.03	0.0515	0.6576	0.0336
	1	1.01±0.03	1.13±0.04			
	7	1.06±0.03	1.02±0.03			
	30*	1.01±0.02	1.16±0.06			
FAC, %	Baseline	42.93±1.99	49.60±2.75	0.0041	0.0004	0.3843
	1	34.05±2.54	39.99±3.06			
	7	35.72±1.96	44.27±2.95			
	30†	33.95±2.20	46.61±3.61			
LV diastolic dimension, mm	Baseline	3.99±0.06	3.90±0.10	0.4113	<0.0001	0.0504
	1	3.69±0.10	3.53±0.16			
	7	3.85±0.11	4.04±0.11			
	30	4.33±0.09	4.03±0.11			
LV systolic dimension, mm	Baseline	2.93±0.08	2.62±0.13	0.2108	<0.0001	0.1092
	1	3.03±0.14	2.65±0.16			
	7	3.09±0.11	3.03±0.14			
	30	3.55±0.11	2.90±0.18			
Anterior wall thickness diastole, mm	Baseline	0.88±0.02	0.88±0.03	0.6982	<0.0001	0.6849
	1	1.08±0.04	1.12±0.05			
	7	0.96±0.05	0.92±0.04			
	30	0.92±0.03	0.97±0.03			

Table 3. Continued

	Days After MI	*Wls^fl/fl* (n=15)	*cfms-icre;Wls^fl/fl* (n=10)	P (Repeated-Measures ANOVA)		
				Wls−/− Effect	Time Effect	Interaction
Anterior wall thickness systole, mm	Baseline	1.18±0.03	1.28±0.06	0.1618	0.3164	0.8124
	1	1.23±0.06	1.31±0.06			
	7	1.16±0.06	1.17±0.06			
	30	1.13±0.03	1.24±0.07			
LV mass, mg	Baseline	121.81±4.22	122.12±7.50	0.7138	<0.0001	0.5013
	1	130.63±8.93	126.91±6.27			
	7	126.50±4.47	128.80±5.22			
	30	150.67±8.04	140.08±4.48			
LV volume, diastole, mm³	Baseline	70.15±2.55	66.59±4.03	0.4200	<0.0001	0.0399
	1	58.93±3.76	53.52±5.48			
	7	65.39±4.58	72.46±4.84			
	30	85.53±4.53	72.32±4.94			
LV volume, systole, mm³	Baseline	33.69±2.19	26.22±3.29	0.0321	<0.0001	0.0333
	1	37.89±3.88	27.39±3.81			
	7	38.84±3.65	37.31±4.54			
	30†	54.02±4.57	34.32±5.16			

Results are presented as mean±SEM. Statistical analysis: 2-way repeated-measures analysis of variance with Bonferroni posttest. 2D indicates 2-dimensional; *cfms*, colony-stimulating factor 1 receptor; FAC, fractional area change; LV, left ventricle; MI, myocardial infarction; *Wls*, Wntless.
*P<0.05, †P<0.01, ‡P<0.001 vs *Wls^fl/fl*.

fibroblasts, myofibroblasts, and epicardial cells[14,16,20,21] but not in macrophages.[21] Furthermore, costaining for β-catenin and macrophages in the infarcted tissue (Figure 1G) suggests that infarct macrophages are nonresponsive to the Wnt/β-catenin pathway. Hence, although different cells in the heart contribute to the canonical Wnt response, we identified infarct macrophages as contributors to the noncanonical response after MI.

Potential Mechanisms: Macrophage Polarization, Angiogenesis, and Protection

Our results suggest several possible mechanisms by which specific *Wls* deletion in macrophages contributes to improved myocardial healing and function after injury. First, loss of Wnt ligand secretion by macrophages was associated with a shift toward an M2-like phenotype and an increase in the M2/M1 ratio in the heart after MI. The importance of the M2 macrophage subset for both angiogenesis and improved myocardial repair after MI has been described by us and others,[2,3,5,37] and the shift toward an M2 phenotype in *Wls*-deficient macrophages fits their proangiogenic and beneficial effect on cardiac healing and remodeling.

The development of the unique phenotype and function of *Wls*-deficient macrophages could be explained by an autocrine mechanism. The noncanonical Wnt5a is an example of an autocrine and paracrine macrophage-derived effector that can switch activated macrophages into a proinflammatory phenotype.[42-44] In the present study Wnt5a was upregulated in infarct macrophages compared with resident sham macrophages. Thus, inhibition of macrophage Wnt5a secretion could have blocked the inflammatory autocrine loop and switched macrophages toward an M2-like phenotype in *cfms-icre;Wls^fl/fl* mice. Subsequently, M2-like macrophages suppressed excessive inflammation and improved infarct repair.[2,3,5,37] However, it is also possible that accumulated Wnt proteins in infarct macrophages drive the M2-like polarization.

Inflammatory cytokine secretion analysis revealed that *Wls*-deficient macrophages have an improved reparative paracrine profile compared with control macrophages. *Wls*-deficient macrophages secrete high levels of VEGF, IL-2, and IL-6, all of which have been shown to be proangiogenic.[45-47] IL-6 is a pleiotropic cytokine with reparative and regenerative properties[48-50] that is also implicated in M2 polarization.[39] In addition, the inhibition of Wnt secretion in macrophages attenuated production of the inflammatory cytokine IL-1α, an important initiator of inflammation in the infarcted heart,[51] and of profibrotic bFGF and IL-13 cytokines.[52,53]

Our transcription analysis also revealed that these macrophages have increased expression of iNOS, which can promote protection from ischemic injury,[54] TGFβ1, a molecule
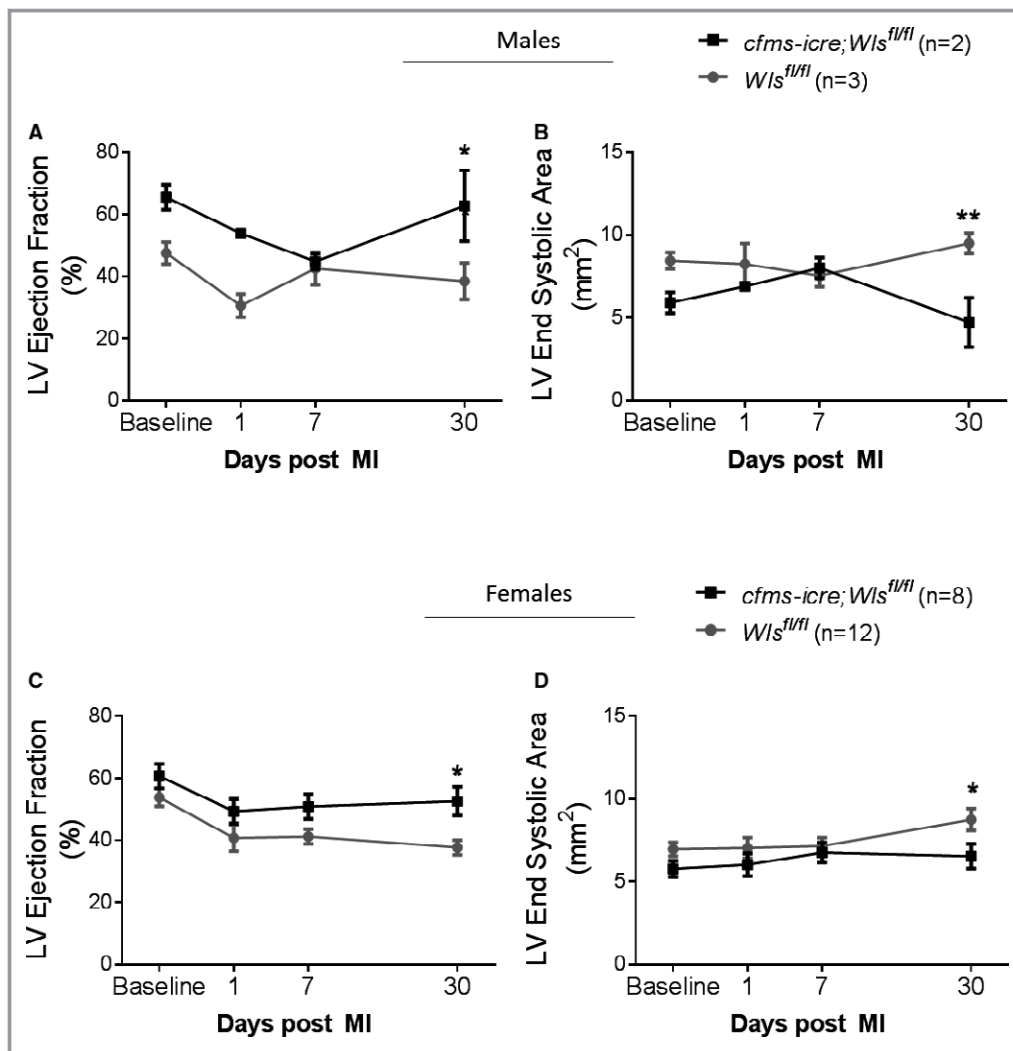
Figure 7. Echocardiography subgroup analysis of male and female *cfms-icre;Wls^fl/fl* and *Wls^fl/fl* mice 30 days after MI. A and B, *Wls* deletion in macrophages improved heart function in the male *cfms-icre;Wls^fl/fl* subgroup compared with *Wls^fl/fl* mice (A) as well as remodeling, determined by LV end systolic area (B), 30 days after MI. C and D, *Wls* deletion in macrophages improved heart function in the female *cfms-icre; Wls^fl/fl* subgroup compared with *Wls^fl/fl* mice (C) as well as LV end-systolic area (D), 30 days after MI. Black line, *cfms-icre;Wls^fl/fl* (n=8 females, 2 males); gray line, *Wls^fl/fl* (n=12 females, 3 males). All results are presented as mean±SEM. Statistical analysis: 2-way repeated-measures analysis of variance with Bonferroni posttest. *$P<0.05$, **$P<0.01$ vs *Wls^fl/fl*. *Cfms* indicates colony-stimulating factor 1 receptor; LV, left ventricle; *Wls*, Wntless.

shown to control infarct healing, resolution of inflammation, ECM deposition, and scar formation,[15,55] and IGF1, which stimulates myocardial repair.[56] Together, our findings demonstrate that inhibition of Wnt signaling by macrophages modulates their paracrine profile, which adds to our knowledge regarding the role of macrophage Wnt pathway responses in the setting of MI.

The improvement observed in cardiac healing and function has also been associated with an increase in small-vessel density near the infarcted area in mice lacking macrophage Wnt ligands. The proangiogenic properties of *Wls*-deficient

macrophages were further confirmed in vitro using a HUVEC tube formation assay. The finding that myeloid Wnts regulate angiogenesis was previously shown in a study by Stefater et al in which the same somatic deletion of *Wls* in retinal myeloid cells caused increased angiogenesis in the deeper layers of the retina.[24] The mechanism suggested for the proangiogenic properties of *Wls*-deleted macrophages was by the elimination of noncanonical Wnt5a secretion, which, under normal conditions, increases the secretion of myeloid VEGF inhibitor-sFLT1.[24] Following this line of evidence, another study by Stefater et al showed that macrophages
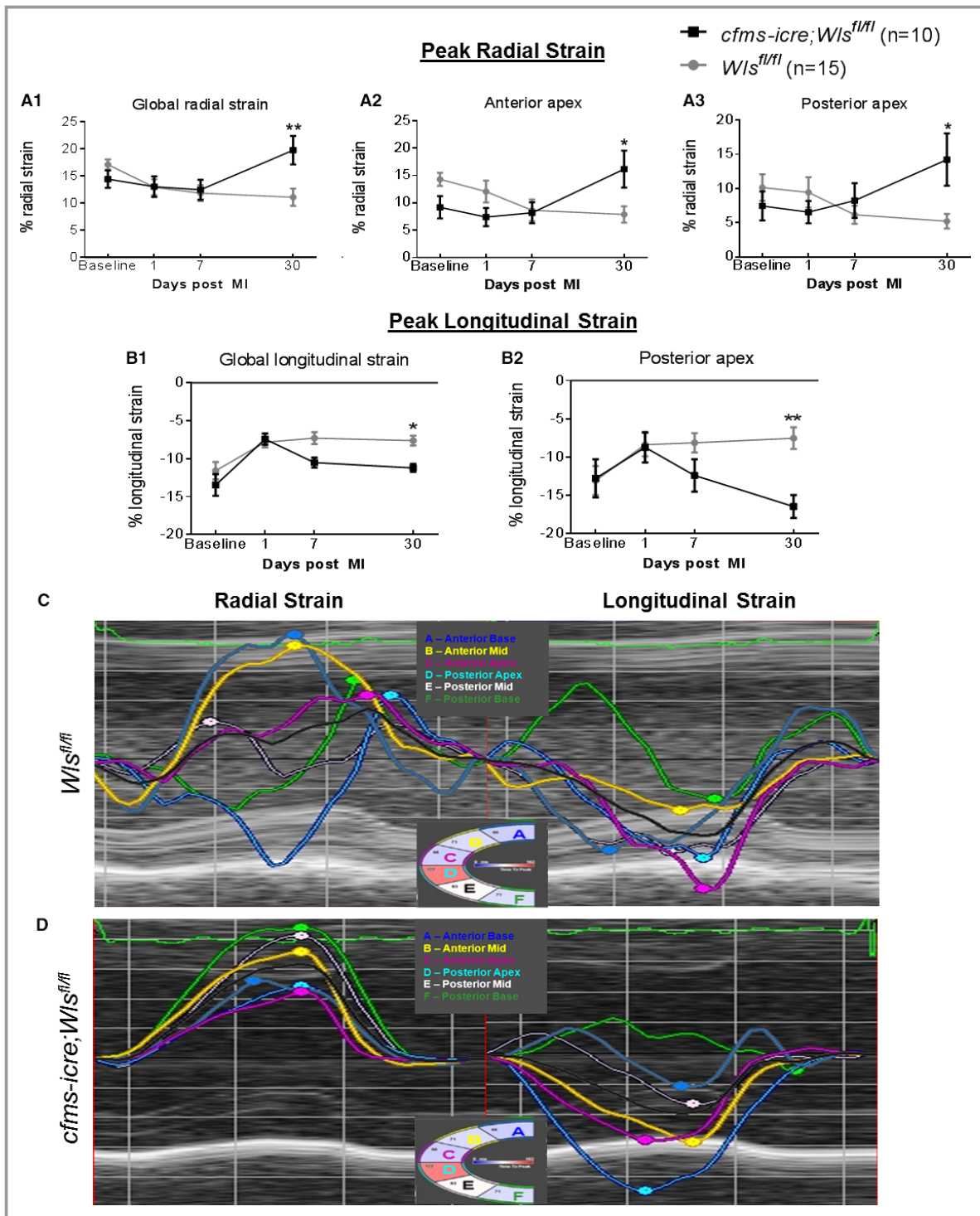
Figure 8. Improved regional and global function in *cfms-icre;Wls^{fl/fl}* mice by speckle-tracking-based strain imaging 30 days after MI. Radial strain in parasternal long-axis view demonstrates improved global (A1) and regional function in the anterior apical (A2) and posterior apical sections (A3) of *cfms-icre;Wls^{fl/fl}*, compared with *Wls^{fl/fl}* mice. B, Longitudinal strain in parasternal long-axis view demonstrates improved global (B1) and posterior apical (B2) function in *cfms-icre;Wls^{fl/fl}* mice compared with *Wls^{fl/fl}* mice (values of longitudinal strain are negative; higher negative numbers indicate greater peak longitudinal strain). C, Representative image of abnormal longitudinal and radial strain curves in *Wls^{fl/fl}* mice 30 days month after MI. D, Representative image of longitudinal and radial strain curves in *cfms-icre;Wls^{fl/fl}* mice 30 days after MI, indicating improved regional function and synchronization compared with *Wls^{fl/fl}* control mice. Black line, *cfms-icre;Wls^{fl/fl}* (n=10); gray line, *Wls^{fl/fl}* (n=15). All results are presented as mean±SEM. Statistical analysis: 2-way repeated-measures analysis of variance with Bonferroni posttest. *$P<0.05$, **$P<0.01$ vs *Wls^{fl/fl}*. Cfms indicates colony-stimulating factor 1 receptor; MI, myocardial infarction; Wls, Wntless.
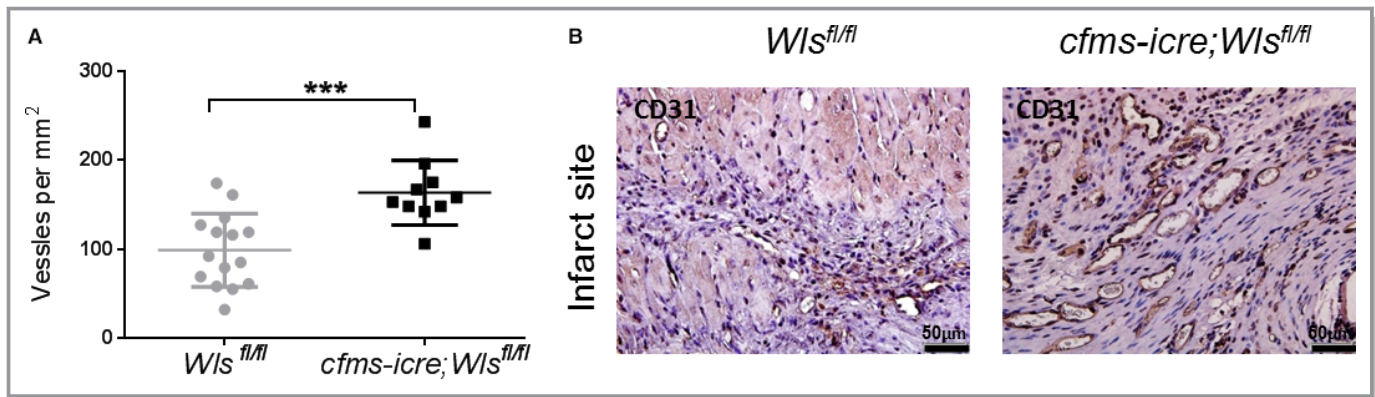
Figure 9. *Wls* deficiency in macrophages increases post-MI angiogenesis. A and B, Histological sections of mouse hearts 1 month after MI, stained for CD31 to count and detect new vessel formation. A, *cfms-icre;Wls*^{fl/fl} mice had 66% more CD31-positive vessels under 20 μm compared with controls. B, Representative images of histological sections of hearts stained against CD31, showing increased vessel density near the infarct in the *cfms-icre;Wls*^{fl/fl} group, ×40 magnification (n=15 in the control group, n=10 in the *cfms-icre;Wls*^{fl/fl} group). Results are presented as mean±SEM. Statistical analysis: two-tailed unpaired Student t test. ***$P<0.001$ vs *Wls*^{fl/fl}. *Cfms* indicates colony stimulating factor 1 receptor; MI, myocardial infarction; *Wls*, Wntless.

Table 4. Morphometric Analysis of Scar Size and Thickness in Midsection of *cfms-icre;Wls*^{fl/fl} and *Wls*^{fl/fl} Mice, 30 Days After MI

	Wls^{fl/fl} (n=15)	*cfms-icre;Wls*^{fl/fl} (n=10)	*P* Value
Relative scar thickness, %	29.7±3.31	30.5±8.31	0.9
Fibrosis (% scar area)	4.5±0.53	4.4±1.28	0.9
Septal thickness, mm	1.1±0.04	1.0±0.07	0.1

LV indicates left ventricular; MI, myocardial infarction; *Wls*, Wntless.
Fibrosis (collagen positive area with Masson trichrome stain) was measured using Sigma Scan Pro planimetry software. % scar area was calculated as scar area (mm^2)/LV muscle area (mm^2), and relative scar thickness was calculated as scar thickness (mm)/septal thickness (mm). Results are presented as mean±SEM. Statistical analysis: 2-tailed unpaired Student t test.

use a Wnt-calcineurin-Flt1 signaling pathway to suppress wound vasculature and delay healing.[12] Taken together, macrophages use the Wnt signaling pathway to control and suppress vascularization in development and wound heal-ing.[12,24] We confirm and extend these findings in a model of acute MI and show that *cfms-icre;Wls*^{fl/fl} hearts develop greater vessel density and improved contractility after MI, compared with *Wls*^{fl/fl} mice.

Finally, small differences in baseline values of contractility and wall thickness between *cfms-icre;Wls*^{fl/fl} and control mice might suggest that *Wls* deletion in macrophages affects myocardial homeostasis under normal conditions. Moreover, some of the favorable effects of *Wls* deletion in macrophages, such as improved ejection fraction, were evident as early as 24 hours after MI (Figure 5). These early effects could indicate that *Wls* deficiency in macrophages also provides myocardial protection. Macrophages populate the infarcted myocardium within 24 hours and peak at 3 to 4 days after

MI.[2,3] *Wls*-deficient macrophages produce several prosurvival factors such as VEGF, IGF, and anti-ischemic NO (Figure 4). Although infarct size was similar in *cfms-icre;Wls*^{fl/fl} and controls, 30 days after MI, we cannot exclude the possibility that *Wls* deletion in macrophages also conferred early myocardial protection during acute MI.

Limitations

Our study has several limitations. First, isolated macrophages in culture display a purification of >90%. Hence, contamina-tion with a small proportion of other cell types other than macrophages, such as cardiac fibroblasts, might have occurred and could have affected the secretome. However, because the same isolation protocol, and hence potential contamination, occurred in both *cfms-icre;Wls*^{fl/fl} and control mice, the differences observed between the groups could most likely be ascribed to *Wls* deletion. Second, when macrophages are being isolated, changes in their activation state and other characteristics can occur. To overcome this problem, we used the minimal plastic adherence time in culture (2 hours) to isolate macrophages. Finally, we have demonstrated the successful recombination of the *Wls* gene in macrophages, but a functional assay measuring the levels of Wnt ligand secretion from *Wls*-deficient macrophages is lacking. We relied on previous work by the Lang lab that demonstrated the absence of noncanonical Wnt secretion from *Wls*-deficient cells.[24]

Conclusions and Implications

We show that the Wnt pathway in macrophages plays a role in defining their inflammatory profile and hence affects the repair process after MI. Our results further suggest a therapeutic

potential in macrophage Wnt pathway modulation to improve cardiac healing and function. There are already several available inhibitors of the pathway such as recombinant soluble frizzled receptors, DKKs, and small molecules designed to block the pathway. Most of these Wnt pathway inhibitors have been tested systemically without targeting a specific cell, which could have decreased their therapeutic potential. Thus, a more specific approach would be to target infarct macrophages in situ with macrophage-targeted carriers loaded with a Wnt secretion inhibitor to improve the outcome of MI.[9,57] Nanocarriers such as liposomes[37] or recombinant high-density lipoprotein[58] can effectively target macrophages in the cardiovascular system. This approach of macrophage Wnt pathway modulation could also be implemented in other macrophage-associated inflammatory diseases.

Acknowledgments

Sources of Funding

Disclosures

None.

References

1. Saxena A, Russo I, Frangogiannis NG. Inflammation as a therapeutic target in myocardial infarction: learning from past failures to meet future challenges. *Transl Res*. 2016;167:152–166.

2. Nahrendorf M, Swirski FK, Aikawa E, Stangenberg L, Wurdinger T, Figueiredo JL, Libby P, Weissleder R, Pittet MJ. The healing myocardium sequentially mobilizes two monocyte subsets with divergent and complementary functions. *J Exp Med*. 2007;204:3037–3047.

3. Ben-Mordechai T, Holbova R, Landa-Rouben N, Harel-Adar T, Feinberg MS, Abd Elrahman I, Blum G, Epstein FH, Silman Z, Cohen S, Leor J. Macrophage subpopulations are essential for infarct repair with and without stem cell therapy. *J Am Coll Cardiol*. 2013;62:1890–1901.

4. Frangogiannis NG. Emerging roles for macrophages in cardiac injury: cytoprotection, repair, and regeneration. *J Clin Invest*. 2015;125:2927–2930.

5. Shiraishi M, Shintani Y, Shintani Y, Ishida H, Saba R, Yamaguchi A, Adachi H, Yashiro K, Suzuki K. Alternatively activated macrophages determine repair of the infarcted adult murine heart. *J Clin Invest*. 2016;126:2151–2166.

6. Frantz S, Hofmann U, Fraccarollo D, Schafer A, Kranepuhl S, Hagedorn I, Nieswandt B, Nahrendorf M, Wagner H, Bayer B, Pachel C, Schon MP, Kneitz S, Bobinger T, Weidemann F, Ertl G, Bauersachs J. Monocytes/macrophages prevent healing defects and left ventricular thrombus formation after myocardial infarction. *FASEB J*. 2013;27:871–881.

7. Aurora AB, Porrello ER, Tan W, Mahmoud AI, Hill JA, Bassel-Duby R, Sadek HA, Olson EN. Macrophages are required for neonatal heart regeneration. *J Clin Invest*. 2014;124:1382–1392.

8. Frangogiannis NG. Inflammation in cardiac injury, repair and regeneration. *Curr Opin Cardiol*. 2015;30:240–245.

9. Ben-Mordechai T, Palevski D, Glucksam-Galnoy Y, Elron-Gross I, Margalit R, Leor J. Targeting macrophage subsets for infarct repair. *J Cardiovasc Pharmacol Ther*. 2015;20:36–51.

10. Weinberger T, Schulz C. Myocardial infarction: a critical role of macrophages in cardiac remodeling. *Front Physiol*. 2015;6:107.

11. Lin SL, Li B, Rao S, Yeo EJ, Hudson TE, Nowlin BT, Pei H, Chen L, Zheng JJ, Carroll TJ, Pollard JW, McMahon AP, Lang RA, Duffield JS. Macrophage Wnt7b is critical for kidney repair and regeneration. *Proc Natl Acad Sci USA*. 2010;107:4194–4199.

12. Stefater JA III, Rao S, Bezold K, Aplin AC, Nicosia RF, Pollard JW, Ferrara N, Lang RA. Macrophage Wnt-calcineurin-Flt1 signaling regulates mouse wound angiogenesis and repair. *Blood*. 2013;121:2574–2578.

13. Gordon MD, Nusse R. Wnt signaling: multiple pathways, multiple receptors, and multiple transcription factors. *J Biol Chem*. 2006;281:22429–22433.

14. Ozhan G, Weidinger G. Wnt/β-catenin signaling in heart regeneration. *Cell Regen (Lond)*. 2015;4:3.

15. Hermans KC, Daskalopoulos EP, Blankesteijn WM. Interventions in Wnt signaling as a novel therapeutic approach to improve myocardial infarct healing. *Fibrogenesis Tissue Repair*. 2012;5:16.

16. Mizutani M, Wu JC, Nusse R. Fibrosis of the neonatal mouse heart after cryoinjury is accompanied by Wnt signaling activation and epicardial-to-mesenchymal transition. *J Am Heart Assoc*. 2016;5:e002457. DOI: 10.1161/JAHA.115.002457.

17. Bao MW, Cai Z, Zhang XJ, Li L, Liu X, Wan N, Hu G, Wan F, Zhang R, Zhu X, Xia H, Li H. Dickkopf-3 protects against cardiac dysfunction and ventricular remodelling following myocardial infarction. *Basic Res Cardiol*. 2015;110:25.

18. Barandon L, Couffinhal T, Ezan J, Dufourcq P, Costet P, Alzieu P, Leroux L, Moreau C, Dare D, Duplàa C. Reduction of infarct size and prevention of cardiac rupture in transgenic mice overexpressing FrzA. *Circulation*. 2003;108:2282–2289.

19. Laeremans H, Hackeng TM, van Zandvoort MA, Thijssen VL, Janssen BJ, Ottenheijm HC, Smits JF, Blankesteijn WM. Blocking of frizzled signaling with a homologous peptide fragment of wnt3a/wnt5a reduces infarct expansion and prevents the development of heart failure after myocardial infarction. *Circulation*. 2011;124:1626–1635.

20. Aisagbonhi O, Rai M, Ryzhov S, Atria N, Feoktistov I, Hatzopoulos AK. Experimental myocardial infarction triggers canonical Wnt signaling and endothelial-to-mesenchymal transition. *Dis Model Mech*. 2011;4:469–483.

21. Duan J, Gherghe C, Liu D, Hamlett E, Srikantha L, Rodgers L, Regan JN, Rojas M, Willis M, Leask A, Majesky M, Deb A. Wnt1/βcatenin injury response activates the epicardium and cardiac fibroblasts to promote cardiac repair. *EMBO J*. 2012;31:429–442.

22. Akhmetshina A, Palumbo K, Dees C, Bergmann C, Venalis P, Zerr P, Horn A, Kireva T, Beyer C, Zwerina J, Schneider H, Sadowski A, Riener MO, MacDougald OA, Distler O, Schett G, Distler JH. Activation of canonical Wnt signalling is required for TGF-β-mediated fibrosis. *Nat Commun*. 2012;3:735.

23. Laeremans H, Rensen SS, Ottenheijm HC, Smits JF, Blankesteijn WM. Wnt/frizzled signalling modulates the migration and differentiation of immortalized cardiac fibroblasts. *Cardiovasc Res*. 2010;87:514–523.

24. Stefater JA, Lewkowich I, Rao S, Mariggi G, Carpenter AC, Burr AR, Fan J, Ajima R, Molkentin JD, Williams BO, Wills-Karp M, Pollard JW, Yamaguchi T, Ferrara N, Gerhardt H, Lang RA. Regulation of angiogenesis by a non-canonical Wnt-Flt1 pathway in myeloid cells. *Nature*. 2011;474:511–515.

25. Bartscherer K, Pelte N, Ingelfinger D, Boutros M. Secretion of Wnt ligands requires Evi, a conserved transmembrane protein. *Cell*. 2006;125:523–533.

26. Port F, Kuster M, Herr P, Furger E, Banziger C, Hausmann G, Basler K. Wingless secretion promotes and requires retromer-dependent cycling of Wntless. *Nat Cell Biol*. 2008;10:178–185.

27. Carpenter AC, Rao S, Wells JM, Campbell K, Lang RA. Generation of mice with a conditional null allele for Wntless. *Genesis*. 2010;48:554–558.

28. Deng L, Zhou JF, Sellers RS, Li JF, Nguyen AV, Wang Y, Orlofsky A, Liu Q, Hume DA, Pollard JW, Augenlicht L, Lin EY. A novel mouse model of inflammatory bowel disease links mammalian target of rapamycin-dependent hyperproliferation of colonic epithelium to inflammation-associated tumorigenesis. *Am J Pathol*. 2010;176:952–967.

29. Muzumdar MD, Tasic B, Miyamichi K, Li L, Luo L. A global double-fluorescent Cre reporter mouse. *Genesis*. 2007;45:593–605.

30. van den Borne SW, van de Schans VA, Strzelecka AE, Vervoort-Peters HT, Lijnen PM, Cleutjens JP, Smits JF, Daemen MJ, Janssen BJ, Blankesteijn WM.

Mouse strain determines the outcome of wound healing after myocardial infarction. *Cardiovasc Res*. 2009;84:273–282.

31. Itzhaki-Alfia A, Leor J, Raanani E, Sternik L, Spiegelstein D, Netser S, Holbova R, Pevsner-Fischer M, Lavee J, Barbash IM. Patient characteristics and cell source determine the number of isolated human cardiac progenitor cells. *Circulation*. 2009;120:2559–2566.

32. Baba T, Ishizu A, Iwasaki S, Suzuki A, Tomaru U, Ikeda H, Yoshiki T, Kasahara M. CD4+/CD8+ macrophages infiltrating at inflammatory sites: a population of monocytes/macrophages with a cytotoxic phenotype. *Blood*. 2006;107:2004–2012.

33. Colston JT, de la Rosa SD, Koehler M, Gonzales K, Mestril R, Freeman GL, Bailey SR, Chandrasekar B. Wnt-induced secreted protein-1 is a prohypertrophic and profibrotic growth factor. *Am J Physiol Heart Circ Physiol*. 2007;293:H1839–H1846.

34. Yu HM, Jerchow B, Sheu TJ, Liu B, Costantini F, Puzas JE, Birchmeier W, Hsu W. The role of Axin2 in calvarial morphogenesis and craniosynostosis. *Development*. 2005;132:1995–2005.

35. Nelson WJ, Nusse R. Convergence of Wnt, β-catenin, and cadherin pathways. *Science*. 2004;303:1483–1487.

36. Gumbiner BM. Regulation of cadherin-mediated adhesion in morphogenesis. *Nat Rev Mol Cell Biol*. 2005;6:622–634.

37. Harel-Adar T, Ben Mordechai T, Amsalem Y, Feinberg MS, Leor J, Cohen S. Modulation of cardiac macrophages by phosphatidylserine-presenting liposomes improves infarct repair. *Proc Natl Acad Sci USA*. 2011;108:1827–1832.

38. Kadl A, Meher AK, Sharma PR, Lee MY, Doran AC, Johnstone SR, Elliott MR, Gruber F, Han J, Chen W, Kensler T, Ravichandran KS, Isakson BE, Wamhoff BR, Leitinger N. Identification of a novel macrophage phenotype that develops in response to atherogenic phospholipids via Nrf2. *Circ Res*. 2010;107:737–746.

39. Adutler-Lieber S, Ben-Mordechai T, Naftali-Shani N, Asher E, Loberman D, Raanani E, Leor J. Human macrophage regulation via interaction with cardiac adipose tissue-derived mesenchymal stromal cells. *J Cardiovasc Pharmacol Ther*. 2013;18:78–86.

40. Yeo EJ, Cassetta L, Qian BZ, Lewkowich I, Li JF, Stefater JA, Smith AN, Wiechmann LS, Wang Y, Pollard JW, Lang RA. Myeloid WNT7b mediates the angiogenic switch and metastasis in breast cancer. *Cancer Res*. 2014;74:2962–2973.

41. Min JK, Park H, Choi HJ, Kim Y, Pyun BJ, Agrawal V, Song BW, Jeon J, Maeng YS, Rho SS, Shim S, Chai JH, Koo BK, Hong HJ, Yun CO, Choi C, Kim YM, Hwang KC, Kwon YG. The WNT antagonist Dickkopf2 promotes angiogenesis in rodent and human endothelial cells. *J Clin Invest*. 2011;121:1882–1893.

42. Pereira C, Schaer DJ, Bachli EB, Kurrer MO, Schoedon G. Wnt5A/CaMKII signaling contributes to the inflammatory response of macrophages and is a target for the antiinflammatory action of activated protein C and interleukin-10. *Arterioscler Thromb Vasc Biol*. 2008;28:504–510.

43. Deb A. Cell-cell interaction in the heart via Wnt/β-catenin pathway after cardiac injury. *Cardiovasc Res*. 2014;102:214–223.

44. George SJ. Wnt pathway: a new role in regulation of inflammation. *Arterioscler Thromb Vasc Biol*. 2008;28:400–402.

45. Felmeden DC, Blann AD, Lip GY. Angiogenesis: basic pathophysiology and implications for disease. *Eur Heart J*. 2003;24:586–603.

46. Bouchentouf M, Williams P, Forner KA, Cuerquis J, Michaud V, Paradis P, Schiffrin EL, Galipeau J. Interleukin-2 enhances angiogenesis and preserves cardiac function following myocardial infarction. *Cytokine*. 2011;56:732–738.

47. Fan Y, Ye J, Shen F, Zhu Y, Yeghiazarians Y, Zhu W, Chen Y, Lawton MT, Young WL, Yang GY. Interleukin-6 stimulates circulating blood-derived endothelial progenitor cell angiogenesis in vitro. *J Cereb Blood Flow Metab*. 2008;28:90–98.

48. Han C, Nie Y, Lian H, Liu R, He F, Huang H, Hu S. Acute inflammation stimulates a regenerative response in the neonatal mouse heart. *Cell Res*. 2015;25:1137–1151.

49. Banerjee I, Fuseler JW, Intwala AR, Baudino TA. IL-6 loss causes ventricular dysfunction, fibrosis, reduced capillary density, and dramatically alters the cell populations of the developing and adult heart. *Am J Physiol Heart Circ Physiol*. 2009;296:H1694–H1704.

50. Zhang C, Li Y, Wu Y, Wang L, Wang X, Du J. Interleukin-6/signal transducer and activator of transcription 3 (STAT3) pathway is essential for macrophage infiltration and myoblast proliferation during muscle regeneration. *J Biol Chem*. 2013;288:1489–1499.

51. Lugrin J, Parapanov R, Rosenblatt-Velin N, Rignault-Clerc S, Feihl F, Waeber B, Muller O, Vergely C, Zeller M, Tardivel A, Schneider P, Pacher P, Liaudet L. Cutting edge: IL-1α is a crucial danger signal triggering acute myocardial inflammation during myocardial infarction. *J Immunol*. 2015;194:499–503.

52. Virag JA, Rolle ML, Reece J, Hardouin S, Feigl EO, Murry CE. Fibroblast growth factor-2 regulates myocardial infarct repair: effects on cell proliferation, scar contraction, and ventricular function. *Am J Pathol*. 2007;171:1431–1440.

53. O'Reilly S, Ciechomska M, Fullard N, Przyborski S, van Laar JM. IL-13 mediates collagen deposition via STAT6 and microRNA-135b: a role for epigenetics. *Sci Rep*. 2016;6:25066.

54. Duranski MR, Greer JJ, Dejam A, Jaganmohan S, Hogg N, Langston W, Patel RP, Yet SF, Wang X, Kevil CG, Gladwin MT, Lefer DJ. Cytoprotective effects of nitrite during in vivo ischemia-reperfusion of the heart and liver. *J Clin Invest*. 2005;115:1232–1240.

55. Chen W, Frangogiannis NG. Fibroblasts in post-infarction inflammation and cardiac repair. *Biochim Biophys Acta*. 2013;1833:945–953.

56. Ruvinov E, Leor J, Cohen S. The promotion of myocardial repair by the sequential delivery of IGF-1 and HGF from an injectable alginate biomaterial in a model of acute myocardial infarction. *Biomaterials*. 2011;32:565–578.

57. Patel SK, Janjic JM. Macrophage targeted theranostics as personalized nanomedicine strategies for inflammatory diseases. *Theranostics*. 2015;5:150–172.

58. Duivenvoorden R, Tang J, Cormode DP, Mieszawska AJ, Izquierdo-Garcia D, Ozcan C, Otten MJ, Zaidi N, Lobatto ME, van Rijs SM, Priem B, Kuan EL, Martel C, Hewing B, Sager H, Nahrendorf M, Randolph GJ, Stroes ES, Fuster V, Fisher EA, Fayad ZA, Mulder WJ. A statin-loaded reconstituted high-density lipoprotein nanoparticle inhibits atherosclerotic plaque inflammation. *Nat Commun*. 2014;5:3065.